Available online at www.sciencedirect.com

SCIENCE DIRECT®

Journal of Solid State Chemistry 179 (2006) 156–160

JOURNAL OF SOLID STATE CHEMISTRY

www.elsevier.com/locate/jssc

Hydrothermal synthesis and characterization of a new three-dimensional hybrid zinc phosphate $[Zn_2(HPO_4)_2(4,4'\text{-bipy})]\cdot 3H_2O$ with neutral porous framework

Lei Wang, Ming Yang, Guanghua Li, Zhan Shi, Shouhua Feng*

State Key Laboratory of Inorganic Synthesis and Preparative Chemistry, College of Chemistry, Jilin University, Changchun 130012, PR China

Received 17 August 2005; received in revised form 6 October 2005; accepted 6 October 2005
Available online 11 November 2005

Abstract

Employing 4,4′-bipyridine as a bridged ligand, a new three-dimensional (3-D) hybrid zinc phosphate $[Zn_2(HPO_4)_2(4,4'\text{-bipy})]\cdot 3H_2O$ has been prepared under hydrothermal conditions and characterized by single crystal X-ray diffraction. This compound crystallizes in the monoclinic space group $C2/c$, with cell parameters, $a = 21.188(4)$ Å, $b = 10.229(2)$ Å, $c = 9.0656(18)$ Å, $\beta = 90.21(3)°$, $V = 1964.8(7)$ Å^3 and $Z = 4$. The connectivity of the ZnO_3N and HPO_4 tetrahedra results in a 2-D neutral layer that with interesting $4,8^2$ net along the bc plane. Furthermore, the 4,4′-bipyridine molecule links the $4,8^2$ net into a 3-D structure. The water molecules sit in the middle of the channels and interact with the framework via hydrogen bonds. The compound exhibits intense photoluminescence at room temperature.

Keywords: Hybrid compound; Neutral framework; Hydrothermal synthesis; Zinc phosphate; Crystal structure

1. Introduction

Recently, many researchers have used a hybrid approach to the syntheses of inorganic–organic open frameworks, in which an organic ligand is combined with an inorganic one, owing to their interesting structural chemistry and potential applications in catalysis, absorbent, and ion exchangers [1–8]. As compared with inorganic ligands such as phosphate and phosphite, the organic ligands have large sizes and a wide variety of means of connection. Accordingly, in this system, a number of zinc phosphates with neutral frameworks have been prepared under hydrothermal condition [9–11]. Lii et al. reported the first metal phosphate incorporating isonicotinate ligand, $Zn(HINT)(HPO_4)$. Its structure consists of 2-D neutral sheets of $Zn(HPO_4)$ with the dipolar isonicotinate ligand being coordinated to zinc as a pendent group [9]. More recently, four new zinc phosphates were synthesized in the presence of D-histidine, 1-methylimidazole, 1,4-bis-(imidazol-1-ylmethyl)benzene, and 1,2-bis(imidazol-1-ylmethyl)benzene, respectively [10]. Each structure is constructed from four-ring secondary building units that consist of two tetrahedral zinc atoms and two tetrahedral phosphate groups. A study of the literature about inorganic–organic hybrid compounds shows that 4,4′-bipyridine (4,4′-bipy) is a good candidate for assembly these compounds, therefore we extended our research into the zinc/4,4′-bipy/H_3PO_4 system [12–19]. In previous work, a novel 3-D zinc fluorophosphates: $Zn_2(4,4'\text{-bipy})(PO_3F)_2$ synthesized under the presence of the fluoride ion has been reported [20]. The fluoride ion not only acts as a mineralizer, but also participates in the formation and structure of the final compound. Herein, in this paper we report another 3-D compound $[Zn_2(HPO_4)_2(4,4'\text{-bipy})]\cdot 3H_2O$ pillared by 4,4′-bipy which was synthesized under hydrothermal conditions but without the fluoride ion.

2. Experimental

2.1. Synthesis and characterization of $[Zn_2(HPO_4)_2(4,4'\text{-bipy})]\cdot 3H_2O$

All chemicals and solvents used in the syntheses were of reagent grade and used as purchased from Beijing without further purification. Compound **1** were prepared from a

---

*Corresponding author. Fax: +86 431 5168624.
E-mail address: shfeng@mail.jlu.edu.cn (S. Feng).

0022-4596/$ - see front matter © 2005 Elsevier Inc. All rights reserved.
doi:10.1016/j.jssc.2005.10.010

mixture of $5ZnO \cdot 2CO_2 \cdot 4H_2O$ (0.567 g, 1 mmol), H_3PO_4 (0.34 ml, 5 mmol), 4,4′-bipy (0.960 g, 5 mmol), and distilled water (10 mL) with a molar composition of 1:5:5:555. The mixture was sealed in a 23 mL capacity of Teflon-lined stainless steel autoclave under autogenous pressure, and heated at 160 °C for 120 h. After cooling colorless crystals for single crystal X-ray diffraction (XRD) were obtained. The yield was 85%, based on Zn. The pH of the reaction mixture before hydrothermal reaction was 2.1. Attempts to synthesize the arsenate analogue under similar reaction were failed.

2.2. General methods

The elemental analyses were performed on a Perkin-Elmer 2400 element analyzer. The inductively coupled plasma (ICP) analysis was carried out on a Perkin-Elmer Optima 3300DV ICP instrument. The infrared (IR) spectrum was recorded within the 400–4000 cm^{-1} region on a Nicolet Impact 410FTIR spectrometer using KBr pellets. Thermogravimetric analysis (TGA) was carried out on a Perkin-Elmer TGA 7 thermogravimetric analyzer in N_2 with a heating rate of 10 °C min^{-1}. The powder XRD patterns were recorded (Bragg–Brentano) on a Siemens D5005 diffractometer by using Cu$K\alpha$ radiation ($\lambda = 1.5418$ Å) with a graphite monochromator. The step size was 0.02° and the count time was 4 s.

2.3. Structure determination

A suitable colorless single crystal with dimensions 0.26 × 0.24 × 0.21 mm was glued to a thin glass fiber and mounted on a Siemens Smart CCD diffractometer equipped with a normal-focus, 2.4-kW sealed-tube X-ray source (graphite-monochromatic Mo$K\alpha$ radiation ($\lambda = 0.71073$ Å) operating at 50 kV and 40 mA. The experiment was conducted at room temperature. Data processing was performed using the SAINT processing program [21]. The total number of measured reflections and observed unique reflections were 9318 and 2219, respectively. Intensity data of 2219 independent reflections ($-27 \leqslant h \leqslant 27$, $-13 \leqslant k \leqslant 13$, $-10 \leqslant l \leqslant 11$) were collected in the ω-scan mode. The structure was solved in the space group $C2/c$ by direct methods and refined on F^2 by full-matrix least squares using SHELXTL97 [22]. The zinc and phosphorus atoms were first located, whereas the carbon, nitrogen, and oxygen atoms were found in the difference Fourier maps. All non-hydrogen atoms were refined anisotropically. The hydrogen atoms residing on the 4,4′-bipy molecules were placed geometrically. The crystallographic data and details on the refinements for the compound are summarized in Table 1. Atomic coordinates and displacement parameters is listed in Table 2.

Table 1
Crystal data and structure refinement parameters for $[Zn_2(HPO_4)_2(4,4'\text{-bipy})] \cdot 3H_2O$

Empirical formula	$C_{10}H_{16}N_2O_{11}P_2Zn_2$
Formula weight	532.93
Temperature	293(2) K
Wavelength	0.71073 Å
Crystal system	Monoclinic
Space group	$C2/c$
a (Å)	21.188(4)
b (Å)	10.229(2)
c (Å)	9.0656(2)
β (deg)	90.21(3)
Volume (Å^3)	1964.8(7)
Z	4
Calculated density (mg/m^3)	1.802
Absorption coefficient (mm^{-1})	2.659
F (000)	1072
Crystal size (mm)	0.26 × 0.24 × 0.21
θ range (deg)	4.16–27.46
Limiting indices	$-27 \leqslant h \leqslant 27$, $-13 \leqslant k \leqslant 13$, $-10 \leqslant l \leqslant 11$
Reflections collected/unique	9318/2219 [R(int) = 0.0270]
Completeness to $\theta = 30.02$	98.7%
Refinement method	Full-matrix least-squares on F^2
Data/restraints/parameters	2219/1/143
Goodness-of-fit on F^2	1.169
Final R indices [$I > 2\sigma(I)$]	$R_1 = 0.0274$, w$R_2 = 0.0809$
R indices (all data)	$R_1 = 0.0306$, w$R_2 = 0.0823$
Largest diff. peak and hole (e Å^{-3})	0.496 and −0.362

Table 2
Atomic coordinates (× 10^4) and equivalent isotropic displacement parameters (Å^2 × 10^3) for $[Zn_2(HPO_4)_2(4,4'\text{-bipy})] \cdot 3H_2O$

Atom	x	y	z	U(eq)[a]
Zn(1)	2766(1)	4303(1)	700(1)	27(1)
P(1)	2219(1)	6574(1)	2633(1)	27(1)
O(1)	2705(1)	6009(2)	1585(2)	34(1)
O(2)	2161(1)	4159(2)	−916(2)	39(1)
O(3)	2626(1)	2999(2)	2154(2)	51(1)
O(4)	1543(1)	6430(3)	1940(2)	53(1)
O(1W)	1492(1)	6553(3)	−931(2)	49(1)
O(2W)	283(4)	5215(10)	−510(12)	58(2)
O(3W)	201(3)	6411(8)	2772(11)	48(2)
N(1)	3625(1)	4234(2)	−285(2)	33(1)
C(1)	3946(2)	3135(3)	−549(4)	54(1)
C(2)	4485(2)	3102(3)	−1392(4)	56(1)
C(3)	4714(1)	4248(3)	−2024(3)	33(1)
C(4)	4385(2)	5385(3)	−1740(4)	44(1)
C(5)	3847(2)	5334(3)	−870(4)	46(1)

[a] U(eq) is defined as one third of the trace of the orthogonalized U_{ij} tensor.

3. Results and discussion

The experimental powder XRD pattern of the bulk product is in good agreement with the simulated one on the basis of the single-crystal structure, as shown in Fig. 1, suggesting the phase purity of the as-synthesized samples. ICP analysis for the product gave the contents of Zn

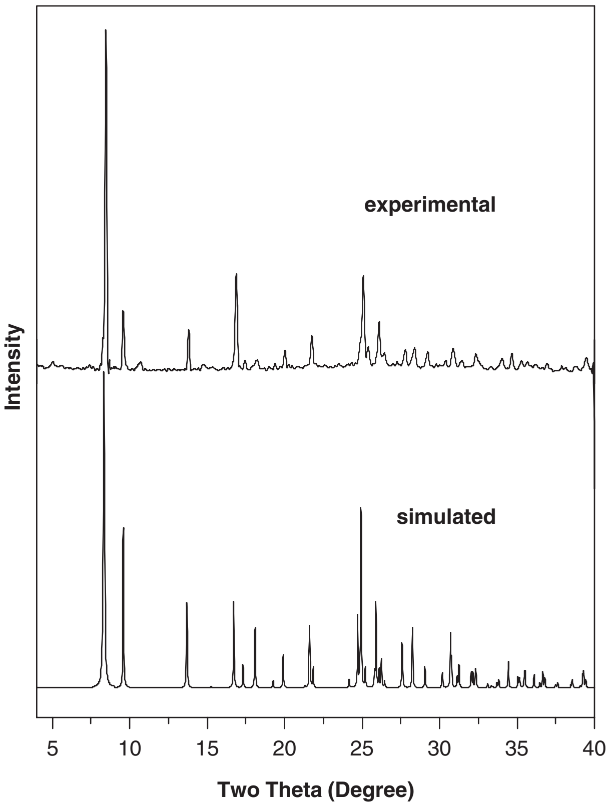

Fig. 1. Simulated and experimental powder X-ray diffraction patterns of the compound.

Table 3
Selected bond lengths (Å) and angles (deg) for $[Zn_2(HPO_4)_2(4,4'\text{-bipy})] \cdot 3H_2O$

Zn(1)–O(3)	1.899(2)	C(4)–C(5)	1.390(4)
Zn(1)–O(1)	1.925(2)	O(3)–Zn(1)–O(1)	109.6(1)
Zn(1)–O(2)	1.949(2)	O(3)–Zn(1)–O(2)	111.4(1)
Zn(1)–N(1)	2.033(2)	O(1)–Zn(1)–O(2)	109.7(1)
P(1)–O(3)#1	1.507(2)	O(3)–Zn(1)–N(1)	115.0(1)
P(1)–O(1)	1.517(2)	O(1)–Zn(1)–N(1)	106.0 (1)
P(1)–O(2)#2	1.519(2)	O(2)–Zn(1)–N(1)	104.7(1)
P(1)–O(4)	1.570(2)	O(3)#1–P(1)–O(1)	107.5(1)
N(1)–C(5)	1.331(4)	O(3)#1–P(1)–O(2)#2	112.6(1)
N(1)–C(1)	1.336(4)	O(1)–P(1)–O(2)#2	114.3(1)
C(1)–C(2)	1.376(4)	O(3)#1–P(1)–O(4)	109.9(1)
C(2)–C(3)	1.393(4)	O(1)–P(1)–O(4)	109.5(1)
C(3)–C(4)	1.380(4)	O(2)#2–P(1)–O(4)	102.9(1)

Symmetry transformations used to generate equivalent atoms: #1: $-x+1/2$, $y+1/2, -z+1/2$; #2: x, $-y+1$, $z+1/2$.

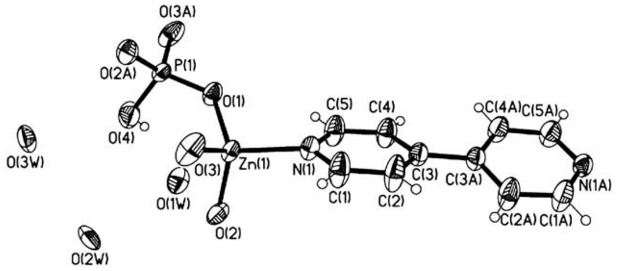

Fig. 2. The building block unit including the asymmetric unit present in the structure (50% thermal ellipsoids).

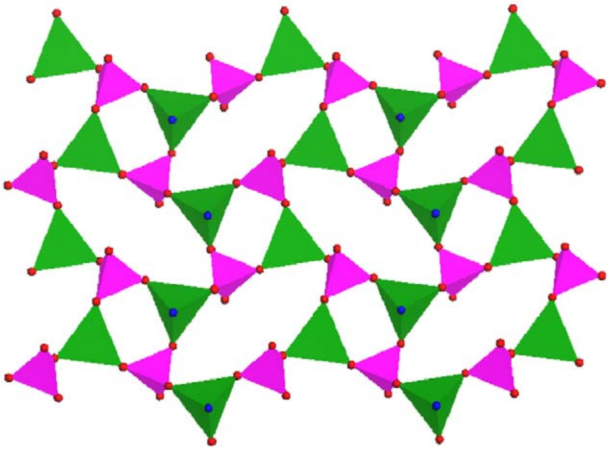

Fig. 3. A View of the 2-D neutral zinc phosphate layer along the *bc* plane showing the $4,8^2$-net sheet. Green, ZnO_3N tetrahedral; Pink, PO_4 tetrahedra.

24.11 wt% (calculated (calcd.) 24.54%) and P 11.23 wt% (calcd. 11.62%), indicating a Zn:P ratio of 1:1. Elemental analyses were consistent with the theoretical values, calcd. for the product: C, 22.54%; H, 3.02%; N, 5.26%. Found: C, 22.15%; H, 2.96%; N, 5.17%. The IR spectrum of the compound showed the vibrations of O–H and C–H bands at ~3500 and 3000 cm^{-1}, and the bands at 1613, 1531, 1482, and 1385 cm^{-1} were assigned to the pyridine ring-stretching vibrations [17,23]. The intense bands in the range 1145–982 cm^{-1} were attributed to the asymmetric and symmetric stretching vibrations of P–O groups [24–26].

The compound crystallizes in the monoclinic space group $C2/c$ with $a = 21.188(4)$ Å, $b = 10.229(2)$ Å, $c = 9.0656(2)$ Å, $\beta = 90.21(3)°$. Selected bond lengths and angles are listed in Table 3. As shown in Fig. 2, the asymmetric unit of it contains 16 unique non-hydrogen atoms, including one zinc atom, one phosphorus atom, seven oxygen atoms, five carbon atoms, and one nitrogen atom. The zinc center coordinates to three oxygen atoms with Zn–O bond lengths in the range 1.899(2)–1.949(2) Å (av. 1.924 Å) and one Nitrogen atoms from 4,4′-bipy with Zn–N bond length 2.033(2) Å. The O–Zn–O angles are in the range 109.6(1)–111.4(1)° (av. 110.2°) and the O–Zn–N angles are in the range 104.7(1)–115.01(1)° (av. 108.3°), which are typical of zinc in the tetrahedral environment. Each phosphorus atom links three adjacent Zn atoms via bridging oxygen. The P–O distances are in the range 1.507(2)–1.570(2) Å (av. 1.528 Å) and O–P–O bond angles are in the range 107.5(1)–114.3(1)° (av. 109.5°). The terminal P(1)–O(4) linkage with a distance of 1.570(2) Å is an –OH group. Bond valence sum calculations on the framework agree with the above results [27].

As shown in Fig. 3, the connectivity of the strictly alternating ZnO_3N and HPO_4 tetrahedra results in a 2-D neutral layer along the *bc*-plane. The neutral layer with

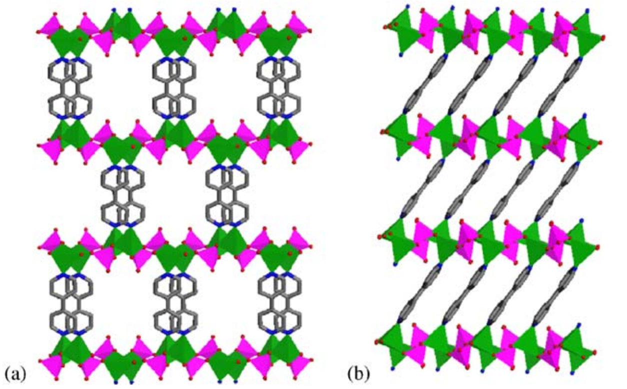

Fig. 4. Crystal structure of $[Zn_2(HPO_4)_2(4,4'\text{-bipy})] \cdot 3H_2O$ viewed along the [001] (a) and [010] (b) directions. Water and hydrogen atoms are omitted for clarity. Green, ZnO_3N tetrahedral; Pink, PO_4 tetrahedra.

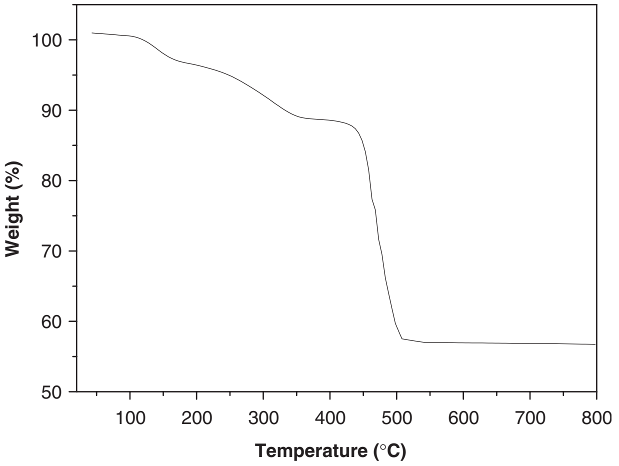

Fig. 5. The TGA curve of $[Zn_2(HPO_4)_2(4,4'\text{-bipy})] \cdot 3H_2O$.

4- and 8-membered rings formed by T atoms ($T = $ Zn, P) can be best described in term of a $4,8^2$ network (each nodal Zn or P atom participates in one 4-ring and two 8-rings), which are stacked along [100] direction in an AAAA sequence. A similar $4,8^2$ network to this compound has been reported in the hybrid zinc/H_3PO_3 system, which contains right-handed and left-handed Zn–O–P helical chains linked together by oxygen atoms, but in the title compound there are no helical chains [23]. Furthermore, the 4,4′-bipyridine molecule links the $4,8^2$ net into a 3-D structure (Fig. 4), giving rise to channels along the [001] and [010] directions. The channel along [001] has dimensions 7.8 × 6.6 Å, Fig. 4(a); for [010] direction is 9.1 × 3.9 Å, Fig. 4(b). The 4,4′-bipy ligand is nearly planar with the two pyridyl rings twisted by 18.3°. The distance between the least-squares planes of adjacent 4,4′-bipy ligands is 9.06 Å, indicating the presence of weak intermolecular aromatic interaction. The water molecules sit in the middle of the channels and interact with the framework via hydrogen bonds.

The initial TGA, performed under flowing N_2, as shown in Fig. 5, exhibits two weight loss stages in the temperature ranges 110–350 and 420–540 °C, corresponding to the concomitant release of composed water (Calcd.: 9.01%; Found: 10.67%) and the decomposition of 4,4′-bipy groups (Calcd.: 33.79%; Found: 32.34%), respectively. The whole weight loss (43.01%) is in good agreement with the calculated (42.80%). At 800 °C, the amorphous phase recrystallized mainly into a $Zn_2P_2O_7$ phase (JCPDS: 73-1648) with some other phase, which was confirmed by powder XRD analysis. To examine the thermal stability of the compound in the release of guest water molecules, a sample of the compound was heated in a thermal gravimetric apparatus at 350 °C for 2 h. Power XRD measurements for the dehydrated product showed that the structure collapsed.

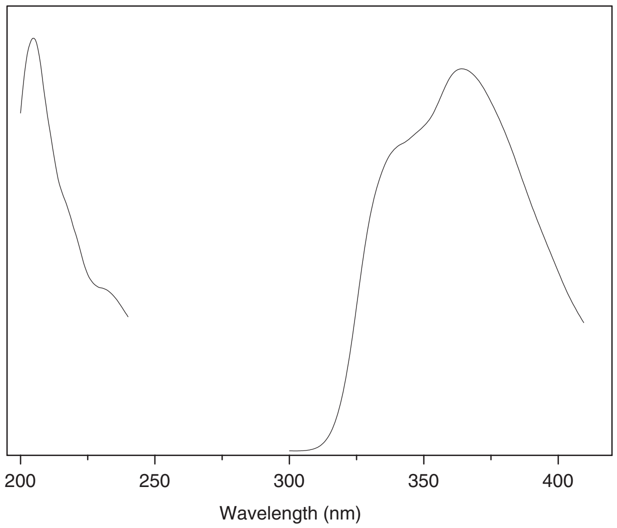

Fig. 6. Solid state excitation-emission spectrum of $[Zn_2(HPO_4)_2(4,4'\text{-bipy})] \cdot 3H_2O$ at room temperature.

The photoluminescence spectrum of the compound was measured in the solid state at room temperature (Fig. 6). On excitation at 207 nm, the emission spectrum for the compound shows a main peak at 365 nm and a shoulder at about 339 nm. The strong emission band at 365 nm is attributable to the $\pi^* \rightarrow n$ transitions of the organic ligand, because a similar emission band at about 369 nm has also been observed on excitation at 254 nm for 4,4′-bipy. The emission at 339 nm can be assigned to ligand-to-metal charge transfer. The strong fluorescent emission of the compound makes it a potentially useful photoactive material, since it is thermally stable and insoluble in common polar and non-polar solvents.

4. Conclusions

A new 3-D hybrid zinc phosphate $[Zn_2(HPO_4)_2(4,4'\text{-bipy})] \cdot 3H_2O$ have been prepared under hydrothermal conditions and characterized by single crystal XRD. The connectivity of the ZnO_3N and HPO_4 tetrahedra results in a 2-D neutral layer that with interesting $4,8^2$ net along the *bc* plane, which are further linked by the 4,4′-bipyridine molecule into a 3-D structure. The water molecules sit in the middle of the channels and interact with the framework via hydrogen bonds. The compound shows intense photoluminescence at room temperature. Further research of this system may focus on the replacement of zinc and 4,4′-bipy with other transition metals and multidentate pyridyl ligands to prepare novel neutral porous compounds and explore their valuable properties.

Acknowledgments

We are grateful to the financial support by the State Basic Research Project and the National Natural Science Foundation of China (No. 20071013).

References

[1] Z.A.D. Lethbridge, P. Lightfoot, J. Solid State Chem. 143 (1999) 58.

[2] J. Do, R.P. Bontchev, A. Jacobson, Inorg. Chem. 39 (2000) 3230.

[3] Z. Shi, L. Zhang, G. Zhu, G. Yang, J. Hua, H. Ding, S. Feng, Chem. Mater. 11 (1999) 3565.

[4] Z.-E. Lin, J. Zhang, Y.-Q. Sun, G.-Y. Yang, Inorg. Chem. 43 (2004) 797.

[5] M.J. Zaworotko, Angew. Chem. Int. Ed. Engl. 37 (1998) 1211.

[6] S.R. Batrten, R. Robson, Angew. Chem. Int. Ed. Engl. 37 (1998) 1460.

[7] T.E. Gier, G.D. Stucky, Nature 349 (1991) 508.

[8] S. Feng, R. Xu, Acc. Chem. Res. 34 (2001) 239.

[9] C.-M. Wang, S.-T. Chuang, Y.-L. Chuang, H.-M. Kao, K.-H. Lii, J. Solid State Chem. 177 (2004) 1252.

[10] J. Fan, C. Slebodnick, R. Angel, B.E. Hanson, Inorg. Chem. 44 (2005) 552.

[11] Z.-E. Lin, Y.-W. Yao, J. Zhang, G.-Y. Yang, J. Chem. Soc. Dalton Trans. (2003) 3160.

[12] L.-H. Huang, H.-M. Kao, K.-H. Lii, Inorg. Chem. 41 (2002) 2936.

[13] L.-I. Hung, S.-L. Wang, H.-M. Kao, K.-H. Lii, Inorg. Chem. 41 (2002) 3929.

[14] Y.C. Jiang, Y.C. Lai, S.L. Wang, K.-H. Lii, Inorg. Chem. 40 (2001) 5320.

[15] C.-Y. Chen, K.-H. Lii, A.J. Jacobson, J. Solid State Chem. 177 (2003) 252.

[16] K.-H. Lii, Y.-F. Hang, Inorg. Chem. 38 (1999) 1348.

[17] Z. Shi, G. Li, D. Zhang, J. Hua, S. Feng, Inorg. Chem. 42 (2003) 2357.

[18] Z. Shi, S. Feng, S. Gao, L. Zhang, G. Yang, J. Hua, Angew. Chem. Int. Ed. 39 (2000) 2325.

[19] Z. Dai, X. Chen, Z. Shi, D. Zhang, G. .Li, S. Feng, Inorg. Chem. 42 (2003) 908.

[20] P.S. Halasyamani, M.J. Drewitt, D. O'Hare, Chem. Commun. (1997) 867.

[21] SMART and SAINT, Siemens Analytical X-ray Instruments, Inc., Madison, WI, 1996.

[22] SHELXTL, Version 5.1, Siemens Industrial Automation, Inc., 1997.

[23] Z.-E. Lin, J. Zhang, S.-T. Zheng, G.-Y. Yang, Micropor. Mesopor. Mater. 68 (2004) 65.

[24] S.B. Harmon, S.C. Sevov, Chem. Mater. 10 (1998) 3020.

[25] S. Natarajan, L.V. Wullen, W. Klein, M. Jansen, Inorg. Chem. 42 (2003) 6265.

[26] Y. Liu, L. Zhang, Z. Shi, H. Yuan, W. Pang, J. Solid State Chem. 158 (2001) 68.

[27] I.D. Brown, D. Altermatt, Acta Crystallogr. B 41 (1984) 244.